1.E.1:
3.A

Nuclear Physics A135 (1969) 116—138; © *North-Holland Publishing Co., Amsterdam*

ANOMALOUS $\frac{5}{2}^+$ AND $\frac{7}{2}^+$ STATES IN ^{99}Rh FROM THE DECAY OF 21 min ^{99}Pd

M. E. PHELPS and D. G. SARANTITES

Department of Chemistry, Washington University, St. Louis, Missouri †

Received 23 May 1969

Abstract: Levels in ^{99}Rh populated in the decay of 21 min ^{99}Pd were investigated. From singles γ-ray energy and intensity measurements employing high-resolution and efficiency Ge(Li) detectors, from coincidence relationships established from γ-γ coincidence experiments employing two Ge(Li) detectors and from β^+-γ coincidence experiments employing a plastic scintillator and a Ge(Li) detector, it was found that levels at 64.6, 200.6, 427.3, 464.3, 851.1, 874.4, 1018.3, 1111.2, 1167.4, 1366.5, 1527.4, 1535.9, 1761.2, 1814.8, 1969.2, 2040.3, 2051.9, 2070.6, 2143.7, 2181.3, 2199.2, 2268.0, 2343.3, 2388.8, 2709.3, 2737.4, 2758.9 and 2835.4 keV are populated in the decay of 22 min ^{99}Pd. Possible levels at 2618.1, 2639.4, 2860.3, 2957.4 and 3047.0 keV are suggested on the basis of energy sums. The fraction of decay of ^{99}Pd to the 16 d ^{99}Rh ground state was determined in milking experiments to be 0.02 ± 0.01 and from the proposed decay scheme, which gives 0.029 ± 0.002. From singles positon spectra and from β^+-γ coincidence measurements, the Q_{EC} value for ^{99}Pd decay was determined to be 3405 ± 20 keV. The half-life of ^{99}Pd was measured to be 21.4 ± 0.2 min. From log ft values obtained and from γ-ray branching information, limits for the J^π values of many levels in ^{99}Rh were placed. The level structure of the "anomalous" $\frac{5}{2}^+$ and $\frac{7}{2}^+$ states in ^{99}Rh is compared with similar levels in other odd-mass Rh isotopes and with recent calculations on the pairing-plus-quadrupole model.

E | RADIOACTIVITY ^{99}Pd; measured E_γ, I_γ, E_{β^+}, γ-γ, β^+-γ, $t_{\frac{1}{2}}$, Q_{EC}. Deduced levels in ^{99}Rh, J^π. Ge(Li), NaI(Tl), plastic scintillation detectors.

1. Introduction

The 21 min ^{99}Pd was first prepared by Aten and De Vries-Hamerling [1]). Its decay was characterized by Katcoff and Abrash [2]), who reported a maximum positon energy of 2.0 ± 0.1 MeV and γ-rays of 140, 275, 420 and 670 keV from measurements employing anthracene and NaI(Tl) scintillators and a gray-wedge coincidence scintillation spectrometer. Although the decay of the neighbouring ^{101}Pd and ^{103}Pd isotopes has been rather well studied in recent years [3,4]), no work other than that of Katcoff and Abrash [2]) could be found in the literature. The levels in ^{99}Rh have not been investigated either from decay of ^{99}Pd or by means of nuclear-reaction studies. Low-lying $\frac{5}{2}^+$ and $\frac{7}{2}^+$ states in nuclei with Z or N equal to 43, 45 and 47 have been termed "anomalous"; attempts have been made by Ikegami and Sano [5]) to explain the nature of these states in terms of the pairing-plus-quadrupole model for the nucleus extended to include admixtures from the next major shell (N or Z equal to 50 to 82).

† Work supported in part by the U.S. Atomic Energy Commission under Contract Nos. AT(11-1) -1530 and AT(11-1)-1760.

Recently, Engels [6]) has attempted to interpret the negative-parity states in a similar nucleus ^{77}Se ($N = 43$) in terms of Nilsson's model [7]) for deformed odd-mass nuclei. As ^{99}Pd has a large Q_{EC} value [2]), it was expected that many low-lying $\frac{3}{2}^+$, $\frac{5}{2}^+$ and $\frac{7}{2}^+$ states in ^{99}Rh would be populated in the decay of 21 min ^{99}Pd. This investigation was undertaken because it was believed that with the aid of high-resolution Ge(Li) γ-ray detectors, the level structure of ^{99}Rh could be well characterized and meaningful comparisons could be made with the above-mentioned models for nuclear structure.

2. Experimental procedures

2.1. PREPARATION OF ^{99}Pd SAMPLES

The ^{99}Pd samples were produced by the ^{96}Ru(^{4}He, n)^{99}Pd reaction using 17 MeV ^{4}He ions from the Washington University cyclotron on natural $RuCl_3$ targets. At this energy, the 17.5 min ^{98}Pd is not expected to be formed. The bombardment times varied between 5 and 20 min, and the beam current was kept below 4 μA in order to avoid decomposition of $RuCl_3$ to the insoluble metal. The targets were mounted on carriers in a pneumatic tube which returned the sources to the counting area in less than 5 sec after the end of bombardment. The most prominent γ-rays of ^{98}Pd were determined in separate experiments by the ^{96}Ru(^{3}He, n)^{98}Pd reaction using 15 MeV ^{3}He ions and were found to be 104, 116, 653 and 665 keV. None of these γ-rays was observed in the spectra attributed to ^{99}Pd.

In all cases, the following radiochemical procedure was employed in order to purify the Pd activity from the products of the (^{4}He, p) and (^{4}He, pn) reactions that are produced in substantial yield.

The $RuCl_3$ target and its 4 mg/cm^2 Al wrapping were dissolved in 2 ml of aqua regia, 5 mg of Pd carrier and 5 mg of Rh holdback carrier were added, and the solution was boiled to near dryness to expel the HNO_3. The solution was diluted with 20 ml of distilled water, and 2 ml of a saturated ethanol solution of dimethylglyoxime (DMG) were added to precipitate the Pd^{II}. The resulting precipitate was filtered and then dissolved in 2 ml of hot conc. HNO_3. The solution was then diluted with 20 ml distilled water, 10 mg of Fe^{III} carrier were added, and $Fe(OH)_3$ was precipitated with NH_4OH to scavenge the remaining Rh and Ru activities. The $Fe(OH)_3$ precipitate was centrifuged and discarded. The supernate was acidified with HCl (until the solution was $\approx 2\,\%$ in HCl) and then boiled for 1 min. To this solution, 5 mg of Rh holdback carrier were added, and Pd^{II} was precipitated with DMG. The precipitate was filtered and mounted for counting.

The decontamination factor of this procedure for the Pd activities from Rh activities was determined in tracer experiments to be $\approx 10^5$. Spectra taken several hours after bombardment showed γ-rays from the daughter 4.7 h ^{99}Rh and from the 8.5 h ^{101}Pd, i.e. the product of the ^{98}Ru(^{4}He, n) reaction. In the γ-ray spectra taken immediately after the Pd separation only the most prominent γ-rays from ^{101}Pd and ^{99m}Rh were observed. Since many samples had to be prepared in each experiment, use of an ^{96}Ru enriched target was not possible.

2.2. DETECTION EQUIPMENT AND METHODS OF COUNTING

For γ-ray counting, both Ge(Li) and NaI(Tl) detectors were employed. The Ge(Li) detectors had active volumes of 20 and 30 cm^3 with FWHM 2.8 and 4.0 keV at the 1332 keV line from a ^{60}Co source, respectively. The detailed description of the dimensions and the properties of these detectors have been given elsewhere [8]). The NaI(Tl) detectors used were integrally mounted 7.6 × 7.6 cm crystals.

For positon counting, a 5.1 cm × 2.6 cm plastic scintillator (pilot B) coupled with a 5.1 cm photomultiplier tube was used.

For the γ-γ coincidence measurements, one NaI(Tl) and either the 30 or the 20 cm^3 Ge(Li) was used. In two other Ge(Li) × Ge(Li) experiments, the 20 and 30 cm^3 Ge(Li) detectors were used. A block diagram of the electronics employed has been given in ref. [8]). The coincidence resolving times employed were typically 100-150 nsec.

The pulse-height analysis system employed has also been described in ref. [8]). Two-parameter coincidence spectra were recorded for each of the NaI(Tl) × Ge(Li) or the 30 cm^3 Ge(Li) × 20 cm^3 Ge(Li) arrangements in a 256 × 1024 channel configuration. The random coincidence events were determined with the aid of a 60 c/sec pulser introduced in one of the preamplifiers as described in ref. [9]). The random events thus determined were found to be insignificant, and they were not subtracted from the spectra shown in the illustrations. Coincidence events resulting from the Compton events of higher-energy γ-transitions were taken into account by taking coincidence spectra on either side of each gated photopeak.

In the β^+-γ coincidence experiments, a 256 × 1024 channel configuration was employed.

The coincidence spectra presented in this work were obtained by adding the coincidence planes to obtain 6 or 12 keV per channel window in the 30 cm^3 Ge(Li) with the use of a read-search unit.

3. Results

To obtain singles γ-ray spectra with good statistics from the decay of the short-lived 21 min ^{99}Pd, many sources (25-35) were employed. The sources were counted for two fixed consecutive time intervals of 15 and 25 min, and the corresponding spectra were added to increase statistics. Comparison of the relative intensities of the γ-peaks from the two timed spectra allowed clear identification of the γ-ray peaks with a half-life of 19-24 min. The very weak γ-rays observed in the spectra taken immediately after separation could not be characterized by half-life. By following samples for decay for a period of 3 d, long-lived γ-peaks were identified with the presence of the daughter 4.7 h ^{99}Rh, the 8.5 h ^{101}Pd from the $^{98}Ru(^4He, n)$ reaction and of very small amounts of 8.1 d ^{100}Pd from the $^{96}Ru(^4He, \gamma)$ reaction. A typical singles γ-ray spectrum obtained by counting 25 samples for a period of 30 min after separation is shown in figs. 1 and 2. In this spectrum, the γ-peaks from the daughter 4.7 h ^{99m}Rh are labelled a, those from 8.5 h ^{101}Pd labelled b and the peaks that were too weak to characterize by half-life labelled c.

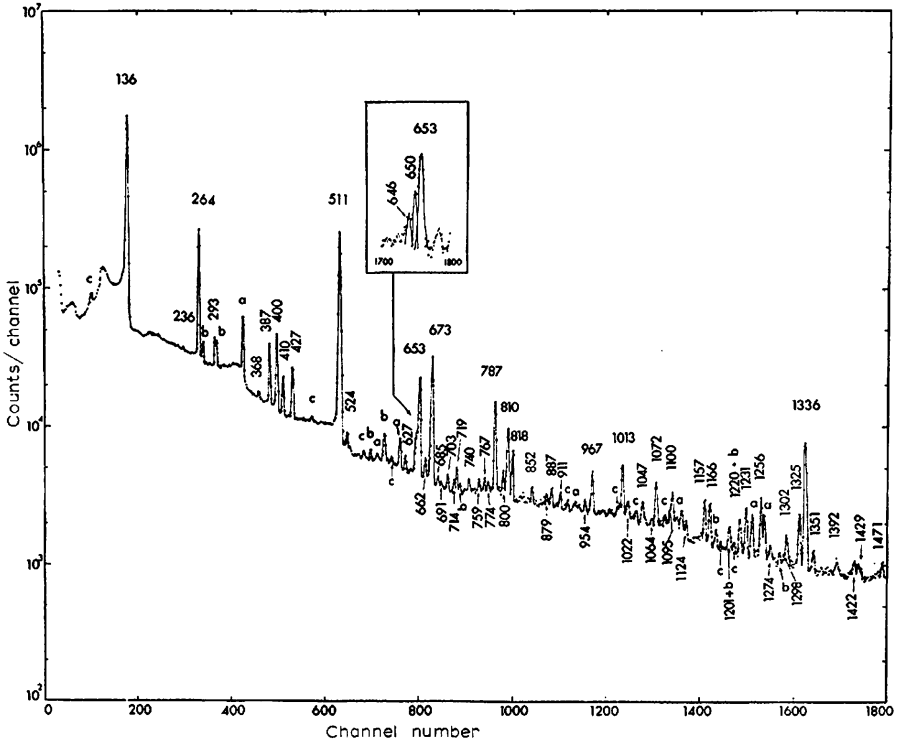

Fig. 1. Lower energy part of the singles γ-ray spectrum following 21 min ^{99}Pd decay obtained by counting 25 samples for a period of 30 min following Pd separation. Peaks labelled a are from 4.7 h ^{99}Rh, those labelled b from 8.5 h ^{101}Pd and those labelled c were too weak to characterize by half-life. The part shown in the insert was obtained in a separate experiment with higher gain.

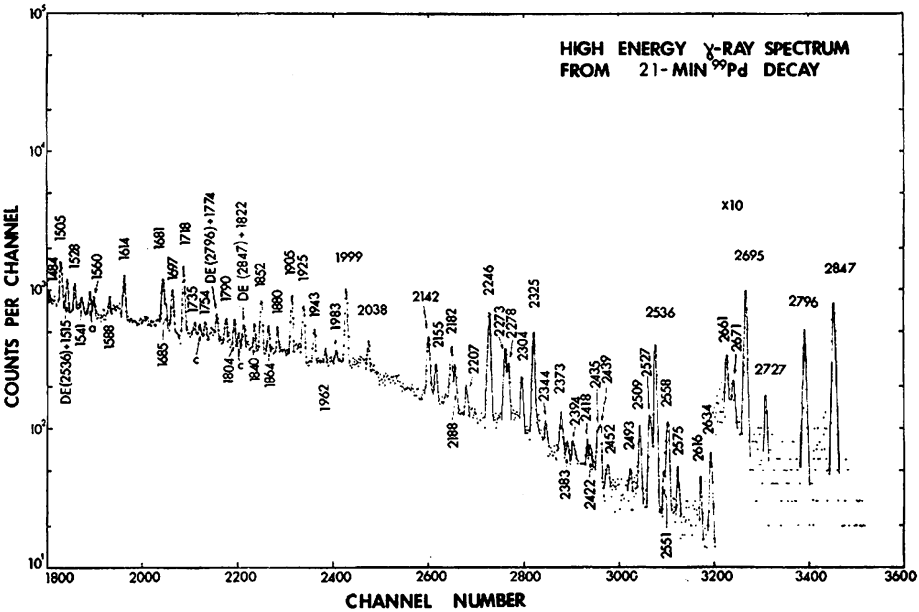

Fig. 2. Higher energy part of the singles γ-ray spectrum following 21 min ^{99}Pd decay (see fig. 1 for comments).

TABLE 1

Energy and intensity of γ-rays following ^{99}Pd decay, from singles measurements

γ-ray energy (keV)		Relative intensity		E_γ from scheme [c]	γ-ray energy (keV)		Relative intensity		E_γ from scheme [c]
136.0	*1*	100.0		136.0	1201.1	*8*	0.15	*6*	1200.8
236.0	*10*	0.23	*4*	236.8	1219.5	*7*	0.41	*10*	1219.5
263.6	*1*	20.9	*10*	263.7	1231.0	*4*	1.0	*1*	1231.5
293.3	*4*	1.8	*3*	293.0	1256.4	*4*	1.4	*2*	
368.0	*3*	0.20	*3*	368.5	1274.2	*8*	0.19	*6*	1272.9
386.7	*1*	3.90	*35*	386.8	1298.0	*8*	0.11	*5*	1296.9
399.8	*1*	4.9	*3*	399.7	1302.2	*7*	0.32	*10* [b]	1301.9
410.3	*2*	1.8	*1*	410.1	1325.0	*5*	1.15	*15*	1324.8
427.3	*1*	2.70	*15*	427.3	1335.6	*4*	6.4	*3*	1335.3
511.0	*1*				1350.9	*10*	0.24	*6*	1350.5
524.1	*2*	0.46	*7*	524.5	1391.6	*10*	0.18	*8*	1392.4
627.0	*4*	0.39	*9*	627.6					1392.6
646.1	*7*	0.81	*6*	646.9	1422.2	*10* [a]	0.22	*10*	1421.5
650.4	*5*	1.8	*2*	650.5	1429.4	*10* [a]	0.27	*10*	1430.0
652.8	*5*	2.0	*2*	653.0	1471.2	*9*	0.31	*9*	1471.3
653.1	*3*	3.5	*2*	653.9	1483.9	*8*	0.17	*7*	
662.4	*4*	0.53	*9*	662.3	1504.8	*5*	0.74	*9*	1504.8
673.4	*2*	9.5	*7*	673.8	1515.1	*8*	0.27	*9* [b]	1514.4
684.8	*4* [a]	0.18	*3*	684.8	1528.1	*6*	0.39	*7*	1527.4
				685.4	1540.8	*10*	0.21	*6*	1541.9
690.5	*6* [a]	0.10	*5*		1559.6	*6*	0.22	*5*	1560.6
702.7	*3*	0.33	*4*	703.1	1587.6	*6*	0.17	*4*	1587.6
714.2	*3*	0.26	*15*		1614.1	*6*	0.66	*8*	1614.2
718.7	*2*	0.59	*6*	718.6	1680.5	*9*	0.85	*15*	1679.4
740.0	*0*	0.23	*4*	740.1	1685.1	*15*	0.21	*8*	
758.5	*4*	0.22	*4*	758.2	1697.3	*6*	0.76	*10*	1696.6
767.2	*5*	0.30	*6*	768.3	1717.6	*5*	0.88	*9*	1717.0
774.0	*6* [a]	0.17	*6*		1735.0	*8*	0.13	*6*	1734.9
786.6	*2*	4.6	*2*	786.5	1754.1	*10*	0.18	*8*	1754.0
800.4	*3*	0.4	*1*		1774.3	*10* [b]	0.15	*8*	
809.8	*2*	2.8	*2*	809.8	1789.6	*10*	0.29	*6*	1790.0
817.6	*2*	1.5	*1*	817.7					1788.3
852.3	*2*	0.42	*8*	852.9	1804.2	*8* [a]	0.24	*8*	1803.7
878.6	*3*	0.33	*6*		1822.2	*9*	0.18	*10* [b]	
886.5	*3*	0.46	*8*	886.8	1840.0	*8*	0.26	*7*	1839.7
				886.8	1851.6	*8*	0.62	*9*	1851.3
910.9	*3*	0.39	*9*	910.6	1863.6	*8*	0.25	*6*	1863.0
954.0	*5*	0.24	*9*	953.7	1879.6	*8*	0.23	*6*	1879.0
967.1	*2*	1.3	*1*	966.8					1879.0
1013.4	*3*	2.0	*2*	1013.9	1904.7	*5*	0.90	*15*	1904.5
1022.1	*3*	0.38	*13*	1022.0	1924.8	*6*	0.65	*10*	1924.5
1046.5	*3*	0.60	*6*	1046.6	1943.4	*7*	0.37	*9*	1943.1
1063.8	*10*	0.10	*4*	1063.1	1962.0	*10*	0.11	*4*	1961.0
1071.7	*3*	1.22	*9*	1071.6	1982.5	*10*	0.08	*3*	1980.7
1095.1	*6*	0.33	*10*	1094.7	1999.1	*5*	1.06	*10*	1998.6
1099.6	*4*	1.4	*2*	1100.1	2037.5	*8*	0.27	*6*	
1124.4	*5*	0.31	*8*	1125.4	2142.4	*7*	0.57	*8*	2142.7
1157.2	*4*	0.91	*15*	1156.8	2154.5	*8*	0.23	*6*	2153.8
1165.6	*4*	1.03	*15*	1165.9	2182.0	*13*	0.41	*9*	2181.3

TABLE 1
(continued)

γ-ray energy (keV)		Relative intensity		E_γ from scheme [c])	γ-ray energy (keV)		Relative intensity		E_γ from scheme [c])
2188.4	*15*	0.28	*8*	2188.2	2508.7	*12*	0.16	*4*	2508.7
2207.3	*10*	0.12	*3*		2527.2	*10*	0.26	*7*	
2246.2	*7*	1.14	*12*	2254.0	2536.3	*9*	0.80	*15*	2536.8
2273.3	*15*	0.48	*15*	2273.1	2550.8	*15*	0.04	*2*	2553.5
2278.2	*15*	0.26	*7*	2278.7	2557.8	*12*	0.26	*8*	2558.3
2304.0	*11*	0.26	*6*		2574.5	*9*	0.04	*1*	2574.8
2324.6	*8*	0.75	*9*	2324.2	2615.8	*10*	0.035	*10*	
2344.4	*15*	0.06	*2*		2633.6	*12*	0.13	*3*	2634.8
2373.1	*11*	0.11	*3*	2371.1	2661.4	*15*	0.056	*10*	2659.7
2382.5	*15*	0.04	*1*		2671.2	*15*	0.014	*10*	2672.8
2394.0	*15*	0.06	*2*	2396.0	2694.9	*10*	0.19	*4*	2694.3
2417.6	*15*	0.035	*15*	2417.5	2726.6	*20*	0.020	*6*	
2421.8	*15*	0.035	*15*		2796.0	*15*	0.12	*3*	2795.7
2434.8	*14*	0.08	*3*		2847.3	*15*	0.21	*6*	2846.4
2439.1	*12*	0.12	*3*	2438.8	2893.0	*20*	0.007	*3*	2892.8
2451.5	*20*	0.04	*1*		2982.0	*20*	0.014	*6*	2982.4
2492.7	*20*	0.03	*1*	2493.1					

[a]) Weak γ-rays assigned to ^{99}Pd decay, for which half-life measurements were not feasible.
[b]) Intensity corrected for contribution from the double-escape peak of a higher-energy γ-ray.
[c]) Energy obtained as weighted average of the energy sums of the γ-rays leading to established levels.

TABLE 2
Energies in keV of the γ-rays contaminating the spectra of the ^{99}Pd samples

4.7 h ^{99m}Rh	8.5 h ^{101}Pd	Weak, unassigned
341	270	74
577	296	461
618	566	554
1116	590	603
1242	724	774
1263	1177	1008
1556	1202 [a])	1035
	1220 [a])	1085
	1289	1184
		1744

[a]) These peaks have ^{99}Pd and ^{101}Pd components.

The energies of the more intense γ-rays from ^{99}Pd decay were determined by counting the ^{99}Pd samples simultaneously with standard sources of ^{57}Co, ^{139}Ce, ^{203}Hg, ^{22}Na, ^{207}Bi, ^{137}Cs and ^{56}Co for calibration. The energy of the weaker γ-rays was obtained from other spectra using the energies of the most intense γ-peaks for internal calibration.

TABLE 3

Summary of the observed coincidence relationships of the γ-rays from ^{99}Pd decay

Fig.	γ-ray in gate (keV)	γ-ray in coincidence (keV)
3a	136 [a]	264, 293, 387, 511, 524, 627, 646, 653, 662, 673, 703, 818, 852, 879, 887, 911, 967, 1013, 1072, 1095, 1124, 1157, 1166, 1201, 1220, 1231, 1325, 1336, 1351, 1505, 1541, 1560, 1588, 1614, 1681, 1685, 1718, 1774, 1840, 1852, 1925, 1943, 1999
	136 [b]	2142, 2246, 2273, 2536, 2558, 2634, 2695
3b	264 [a]	136, 293, 387, 410, 511, 627, 646, 653, 662, 703, 1064, 1072, 1157, 1201, 1220, 1256, 1351, 1505, 1588, 1681, 1718, 1735, 1925
	264 [b]	703, 2246, 2273
4a	293 [a]	136, 264, 400 [c], 673, 810, 1013
4b	387 [a]	136, 264, 400, 511, 1220
5a	400 [a]	387, 410, 511, 646, 1072, 1157, 1220, 1505
	(368, 387, 400, 410, 427) [b]	387, 400, 410, 511, 646, 703, 800, 852, 1072, 1095, 1100, 1157
5b	410 [a]	136, 264, 368, 400, 653 [c]
5c	427 [a]	740, 1013, 1100
6a	511 [a]	136, 264, 387, 400, 650, 673, 787, 810, 818, 1336
	511 [b]	136, 264, 387, 400, 650, 673, 787, 810, 818, 967, 1220, 1336
7a	646 [a]	136, 264
7b	650, 653 [a]	136, 511, 524 [c], 653 [c], 673 [c], 810 [c]
7c	653 [a]	136, 410 [c], 427 [c], 511 [c], 524, 652.8, 673, 810, 1100 [c]
8a	673 [a]	136, 293, 511, 524, 653, 1013, 1095
	(646, 650, 653, 662, 673) [b]	136, 293, 511, 524, 653, 673, 810, 886, 1013, 1095, 1100, 1157, 1166, 1256, 1325
	740 [a]	427
	787 [a]	511
	810 [a]	293, 653, 887, 1013
	818 [a]	136
	911 [a]	136
	(787, 800, 810, 818, 852, 879, 887) [b]	136, 264, 293, 511, 653, 673 [c], 767, 810, 887, 1013, 1022, 1095, 1124, 1325, 1336
	967 [a]	136, 1013
	1013 [a]	136, 264, 293, 400, 410, 427, 673, 703, 740, 967
	(911, 954, 967, 1013) [b]	136, 264, 293, 400, 410, 427, 673, 703, 740, 967, 1013, 1022
	1072 [a]	136, 264, 400
	1100 [a]	427, 524
	(1022, 1047, 1064, 1072, 1095, 1100, 1124) [b]	136, 264, 400, 427, 511, 524, 653 [c], 673 [c], 810, 818, 1157, 1256
	1157 [a]	136, 264, 400
	1166 [a]	136
	1336 [a]	136, 662
	(1124, 1157, 1166, 1201, 1220, 1231) [b]	136, 264, 386, 400, 410, 427 [c], 511 [c], 653, 673, 787, 810, 818,1100
	(1256, 1274, 1298, 1302, 1325, 1336, 1351) [b]	136, 264, 400, 410, 511 [c], 673, 810, 1047
	(1505, 1515, 1528, 1541, 1560) [b]	136, 264, 293, 653, 767
	(1588, 1614, 1681, 1685, 1697) [b]	136, 264, 400, 627
	(1718, 1735, 1754, 1774, 1790, 1804) [b]	136, 264, 293, 400, 427

[a]) From Ge(Li)-Ge(Li) coincidence experiments.

[b]) From NaI-Ge(Li) coincidence experiments.

[c]) Weak coincidence.

The relative efficiencies of the γ-rays were determined from full-energy peak areas using detector efficiency curves obtained by means of standard sources of ^{109}Cd, ^{57}Co, ^{203}Hg, ^{137}Cs, ^{180m}Hf, ^{133}Ba, ^{207}Bi, ^{88}Y and ^{56}Co. The relative intensities of these photons used were from ref. [4]), p. 563.

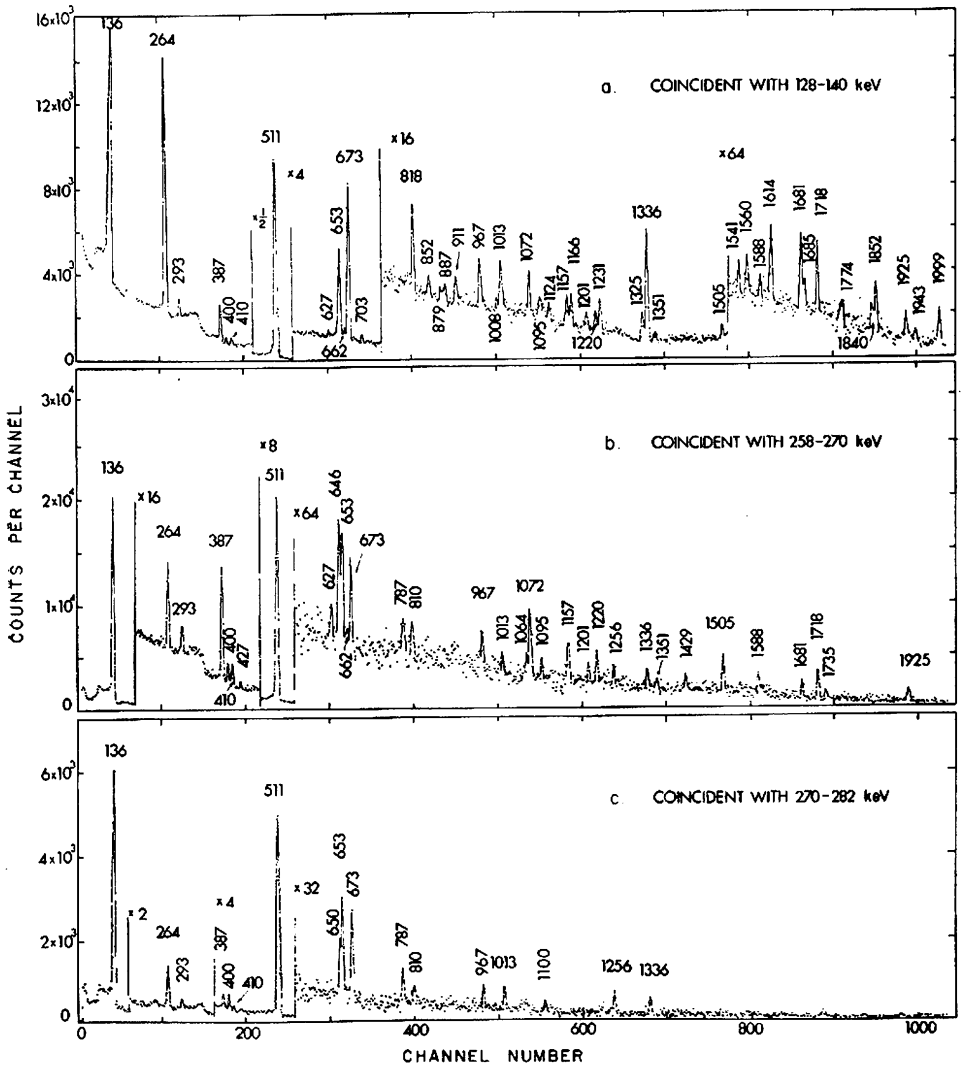

Fig. 3. Spectra of the γ-rays from ^{99}Pd decay observed with the 20 cm^3 Ge(Li) detector in coincidence with the indicated energy regions in the 30 cm^3 Ge(Li) detector. The selected gate in part a contains the 136 keV γ-peak, the gate in part b contains the 264 keV γ-peak and part c displays the contribution from Compton scattered higher energy γ-rays.

The energies and the relative intensities of the γ-rays from ^{99}Pd thus determined from nine different experiments are summarized in table 1. The energies of the γ-rays

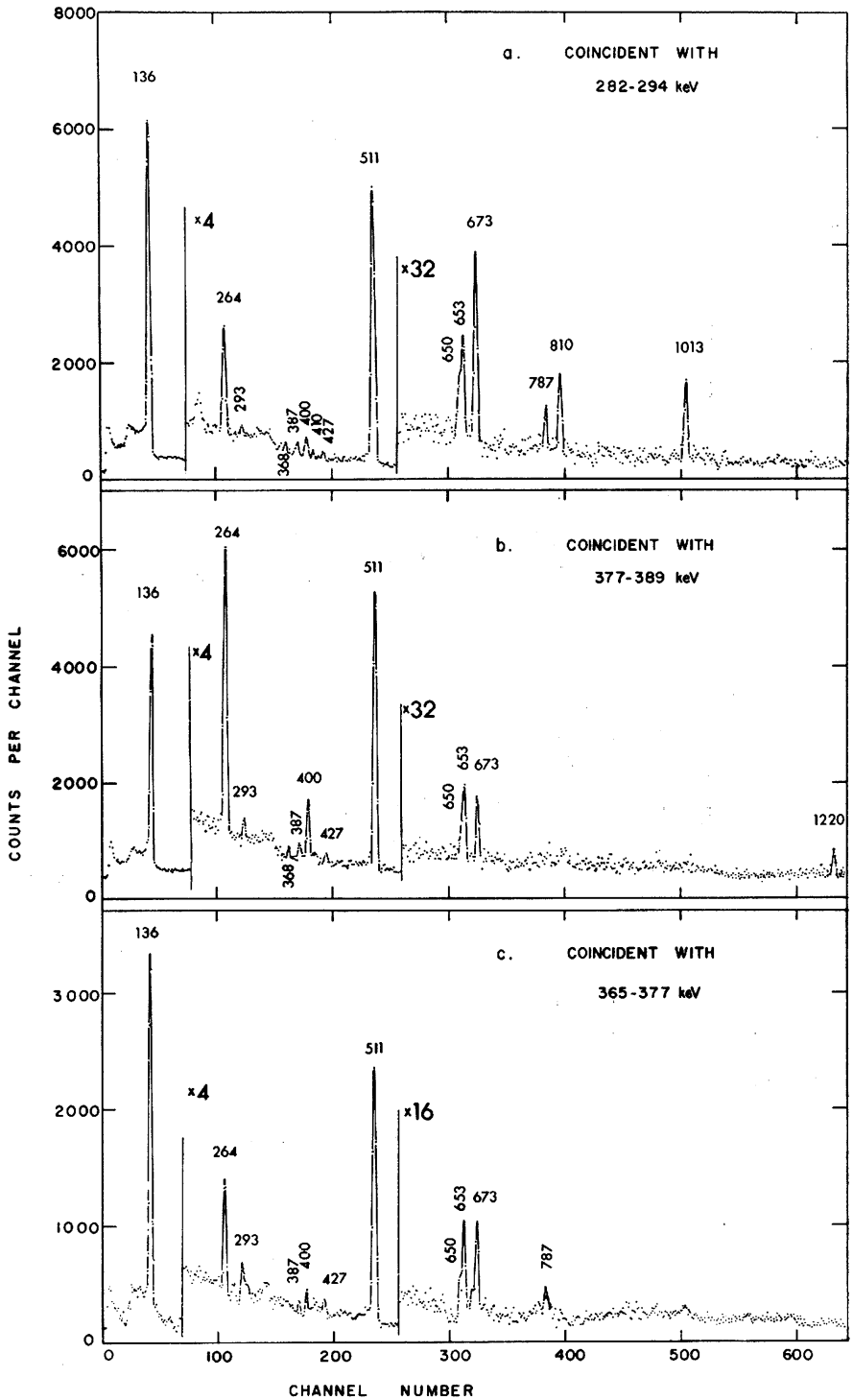

Fig. 4. Spectra of the γ-rays from ^{99}Pd decay observed with the 20 cm^3 Ge(Li) detector in coincidence with the indicated energy regions in the 30 cm^3 Ge(Li) detector. The selected gate in part a includes the 293 keV γ-peak, the gate in part b includes the 387 keV γ-peak and part c shows the contribution from Compton scattered higher energy γ-rays.

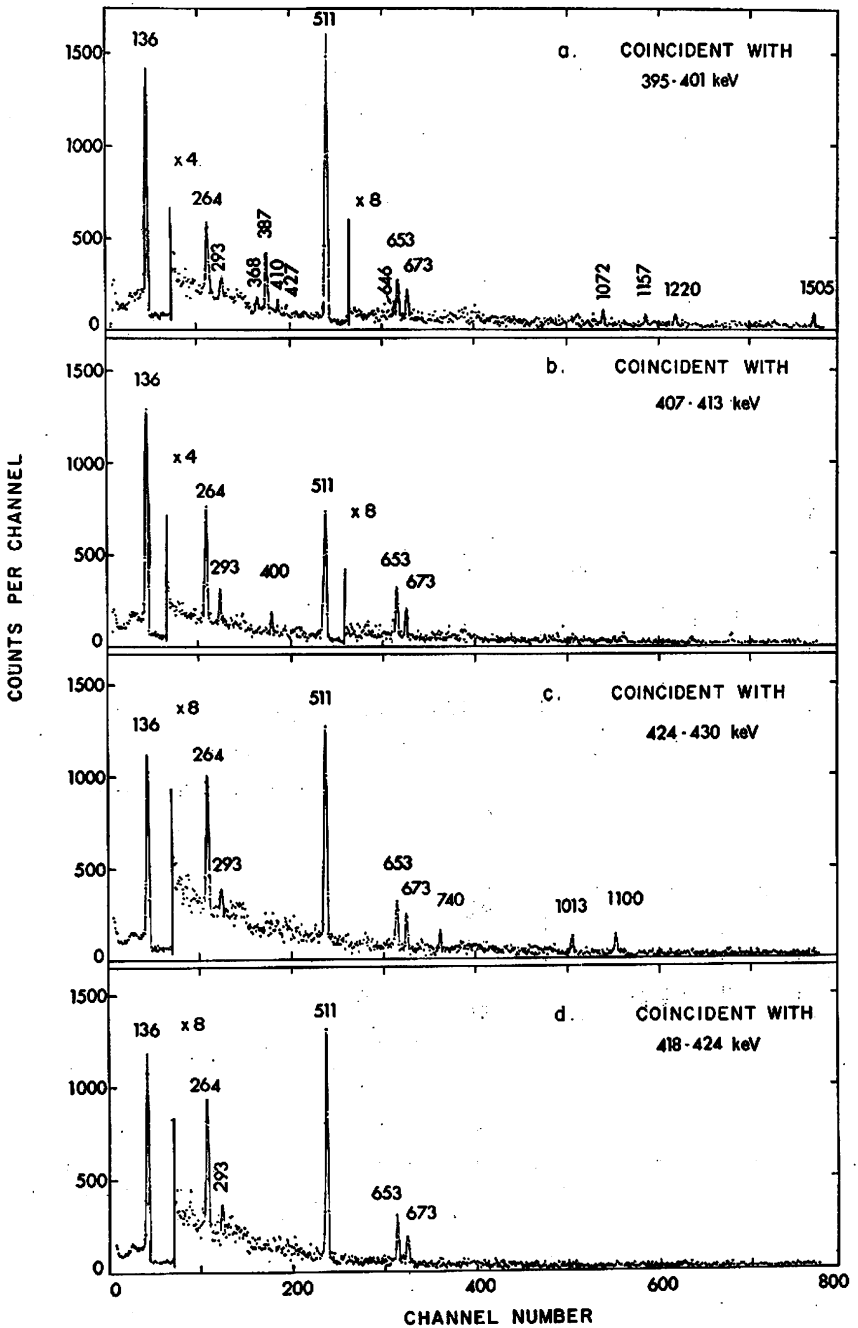

Fig. 5. Spectra of the γ-rays from ^{99}Pd decay observed with the 20 cm^3 Ge(Li) detector in coincidence with the indicated energy regions in the 30 cm^3 Ge(Li) detector. Gate a includes the 400 keV γ-peak, gate b the 410 keV γ-peak, gate c the 427 keV γ-peak and gate d the Compton background.

seen in the ^{99}Pd spectra from ^{99m}Rh, ^{101}Pd and those that were not identified by half-life are listed in table 2.

The half-life of ^{99}Pd decay was redetermined by gross beta counting using a 2π gas-flow proportional counter. The decay curves were analysed by the least-squares method and the average half-life from three independent determinations was found

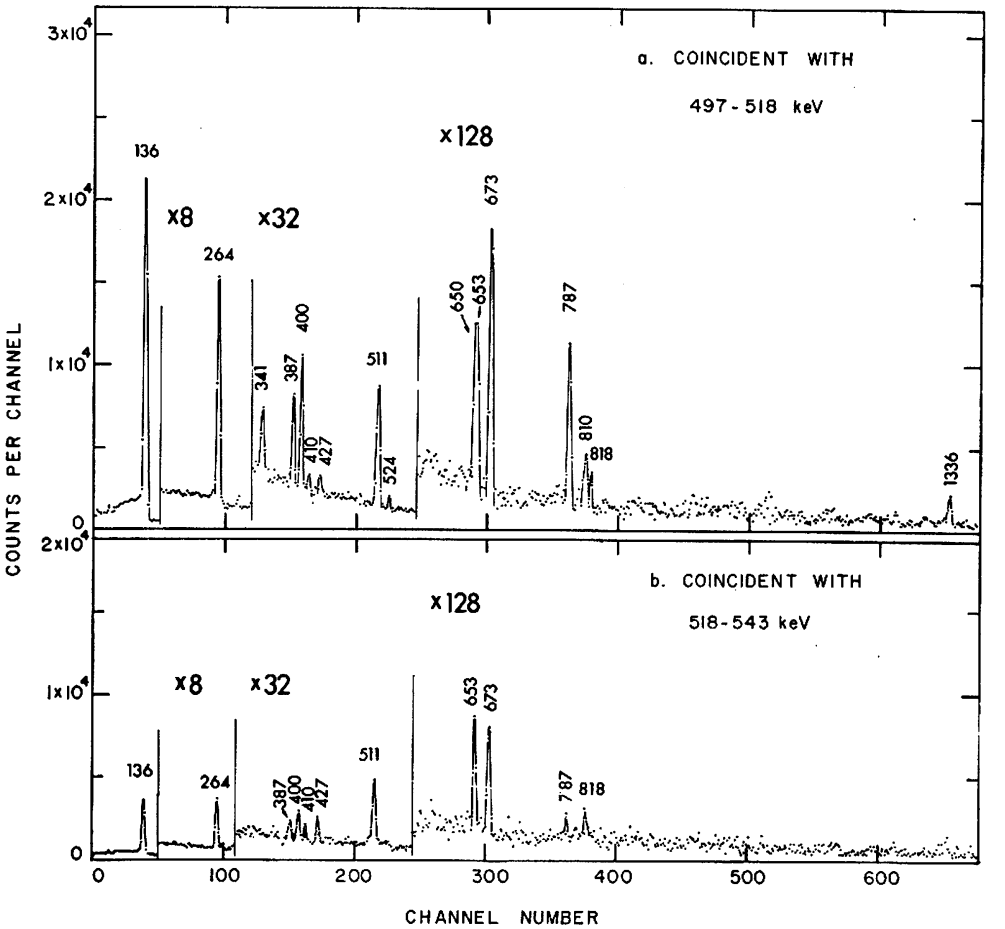

Fig. 6. Spectra of the γ-rays from ^{99}Pd decay observed with the 20 cm^3 Ge(Li) detector in coincidence with the indicated energy regions in the 30 cm^3 Ge(Li) detector. Gate a includes the 511 keV peak of the annihilation radiation and gate b the Compton background.

to be 21.26 ± 0.15 min. In another two experiments, the 136 keV γ-ray peak was followed for decay using a 7.6×7.6 cm NaI(Tl) detector, a single-channel analyser and a scaler. The value of 21.69 ± 0.20 was obtained as a weighted average from two independent measurements. The adopted value is 21.4 ± 0.2 min.

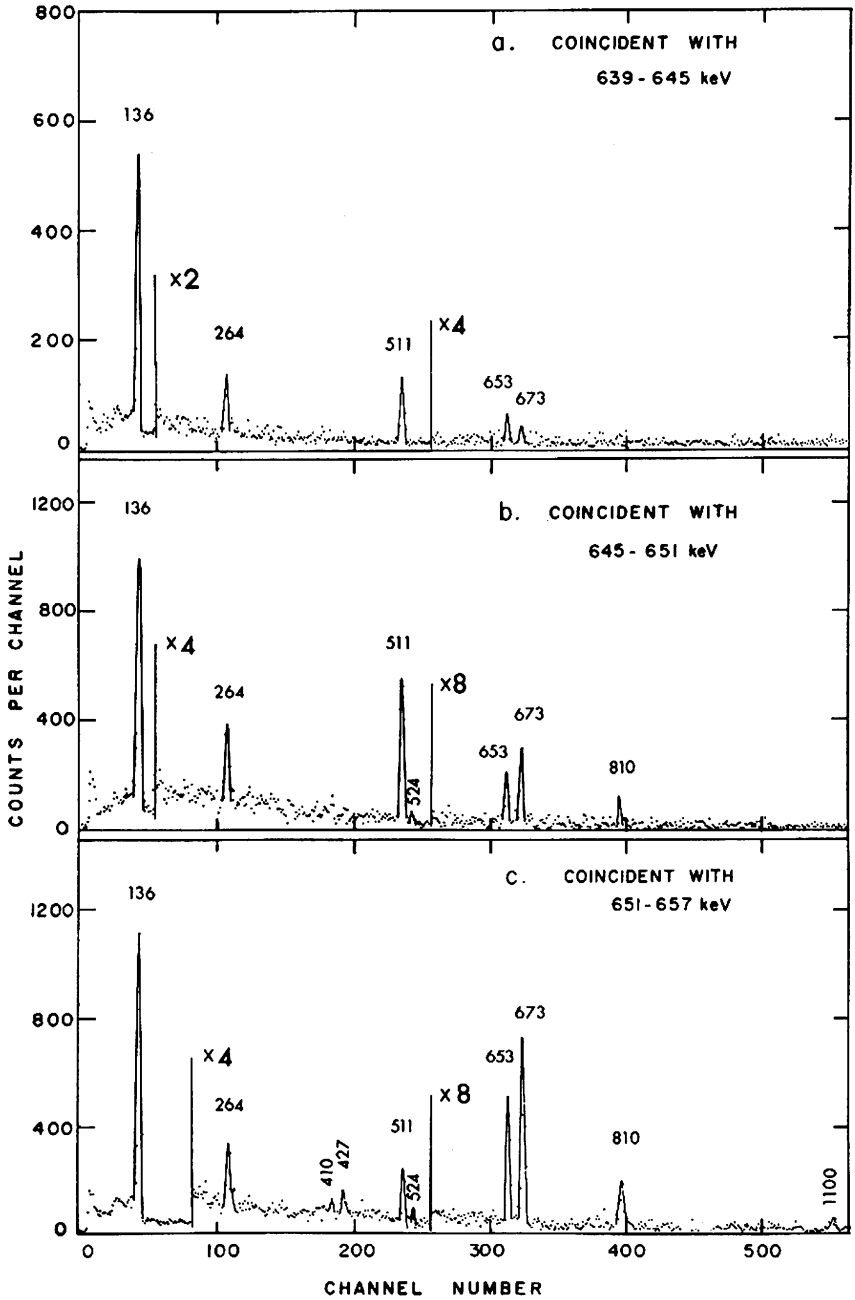

Fig. 7. Spectra of the γ-rays from ^{99}Pd decay observed with the 20 cm^3 Ge(Li) detector in coincidence with the indicated energy regions in the 30 cm^3 Ge(Li) detector. Gate b includes part of the 646 and the 650 keV γ-peaks, gate c includes the 653 keV γ-peak and gate a represents the Compton background.

The fraction of decay of ^{99}Pd to the 16.1 d ground state of ^{99}Rh was determined in the following way. Samples of $RuCl_3$ were bombarded with 17 MeV ^{4}He ions for about 40 min. The 21 min ^{99}Pd activity produced was separated and purified from the Rh activities as described in subsect. 2.1. The sample of ^{99}Pd was then allowed to decay for 60 min, and the Rh activity was then separated by precipitating $K_3Rh(NO_2)_6$. The γ-ray activity was followed for decay using a Ge(Li) detector for a period of 3 d. From the measured intensity of the 90 and 341 keV γ-rays of the 16.1 d ^{99}Rh and

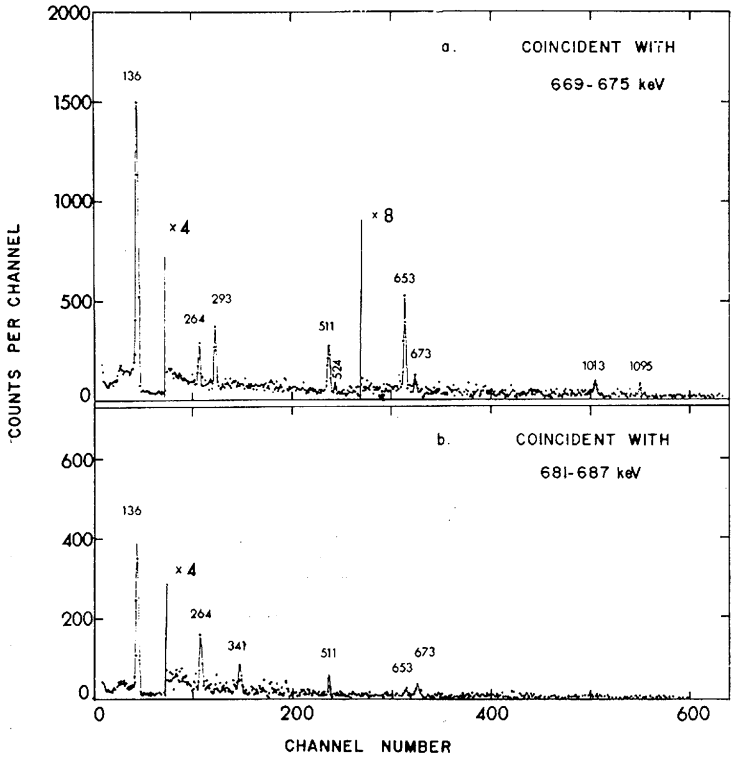

Fig. 8. Spectra of the γ-rays from ^{99}Pd decay observed with the 20 cm^3 Ge(Li) detector in coincidence with the indicated energy regions in the 30 cm^3 Ge(Li) detector. Gate a includes the 673 keV γ-peak and gate b the corresponding Compton background.

4.7 h ^{99m}Rh, respectively, the number of atoms formed as ^{99}Rh and ^{99m}Rh was calculated at the time of separation. The fraction of decay to the 16.1 d ^{99}Rh was thus found to be 0.02 ± 0.01. This value is based on the intensity of the above-mentioned γ-rays listed in ref. [3]). A better value for this fraction, which is consistent with the above measurement, is 0.029 ± 0.002; it is based on the proposed decay scheme.

The coincidence relationships of the γ-rays from ^{99}Pd were established in two two-parameter NaI × Ge(Li) experiments covering the energy ranges (0-2.0) × (0-3.0) MeV, and in two separate two-parameter Ge(Li) × Ge(Li) experiments covering the energy

ranges (0-1.4) × (0-2.1) MeV. The results are summarized in table 3. For purposes of illustration, coincidence spectra shown in figs. 3-8 were chosen only from the Ge(Li) × Ge(Li) experiments because of the reduced complexity of the spectra obtained by gating on only one γ-ray at a time.

The end-point energy of the highest-energy positon group determined by means of a Fermi-Kurie plot (fig. 9a) of the singles total positon spectrum recorded by means of a plastic scintillator was 2180±20 keV. For energy calibration, use was made of

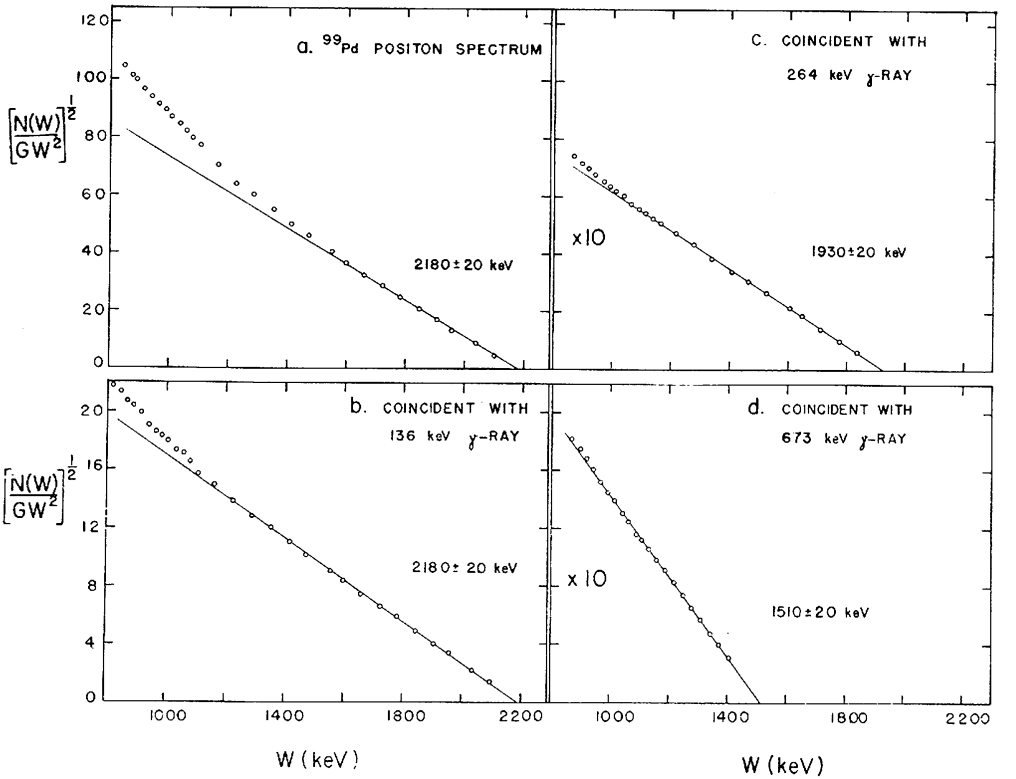

Fig. 9. Fermi-Kurie plots of the positon spectra from ^{99}Pd decay. Part a shows the singles positon spectrum, parts b, c, and d show the positon spectra coincident with the 136, 264 and 673 keV γ-rays.

the conversion electrons from a ^{207}Bi source and the positons from the 69 min ^{101m}In and 9.8 min ^{62}Cu sources with end-point energies of 2.20 and 2.90 MeV, respectively[10,11]). The above value was confirmed by the end-point energies 2180±20, 1930±20, 1580±50 and 1510±20 keV for the highest-energy positon groups obtained in coincidence with the 136, 264, 387 and 673 keV γ-rays (figs. 9b-d). These positon groups are shown below to populate levels at 200.6, 464.3, 851.1 and 874.4 keV in ^{99}Rh, thus establishing the Q_{EC} value for the decay of ^{99}Pd to ^{99}Rh as 3405±20 keV.

4. Construction of the decay scheme

The proposed decay scheme is shown in fig. 10 and below arguments are given for its construction.

The 16.1 d and 4.7 h states in ^{99}Rh have been assigned [3]) as $\frac{1}{2}^-$ and $\frac{9}{2}^+$, respectively. Furthermore, the 16.1 d and 4.7 h states in ^{99}Rh were assigned as the ground state and first excited state at $\approx$ 50 keV on the basis of the positon end-point measurements of Katcoff and Abrash [2]) and of Townley *et al.* [10]). The energy of the 4.7 h state is established at 64.6 keV because the rather intense 427 keV γ-ray was seen only in coincidence with the weak γ-rays at 740, 1100 and 1754 keV, which are shown below to de-excite levels at 1167.4, 1527.4 and 2181.3 keV (see fig. 10). The γ-ray at 136 keV is the most intense, and it was seen in coincidence with a wealth of γ-rays (see table 3 and fig. 3a), which have a sum of intensities not exceeding its intensity. Since ^{99}Pd decays only by 2.9 % to the 16.1 d ground state, the intense 136 keV γ-ray must populate the 4.7 h isomeric state directly, thus establishing a level at 200.6 keV.

The second most intense γ-ray at 264 keV is in strong coincidence with a wealth of γ-rays (table 3 and fig. 3b) including the γ-ray at 136 keV. The 400 keV γ-ray is not in coincidence with the 136 keV γ-ray, but it is seen in coincidence with the 387 keV γ-ray, which is the next most intense γ-ray coincident with the 264 keV γ-ray (see table 3 and fig. 5a). This evidence firmly establishes a level at 464.3 keV with the 400 keV γ-ray populating the 64.6 keV isomeric state.

The 387 keV γ-ray is seen in strong coincidence only with the γ-rays at 136, 264, 400 and 1220 keV (fig. 4b), and because of its high intensity, it must populate the 464.3 keV level directly, thus establishing a level at 851.1 keV. This level is confirmed by the 650 keV γ-ray seen in coincidence with the 136 keV γ-ray and thus assigned to populate the 200.6 keV level; and by the 787 keV cross-over transition assigned on the basis of energy sums to populate the 64.6 keV metastable state. The above assignments are further confirmed by the observed strong coincidence of the 387, 650 and 787 keV γ-rays with the annihilation radiation (figs. 6a and b).

The coincidence of the 1220 keV γ-ray with the 387 keV γ-ray mentioned above (see fig. 4b) suggests a possible level at 2070.6 keV, which could possibly be confirmed by a weak population of this level by an 887 keV γ-ray (fig. 10).

The 673 γ-ray, which is the third most intense, is seen in strong coincidence with the γ-rays at 136, 293, 524, 653, 1013 and 1095 but not with the γ-ray at 264 keV (figs. 3a, 3b and 8a). This strongly suggests a level at 874.4 keV, which is confirmed (i) by the coincidence of the 673 keV γ-ray with a positon group of 1510$\pm$20 keV end-point energy (fig. 9d), (ii) the coincidence of the 410 keV γ-ray with the 136, 264 and 400 keV γ-rays (figs. 3a, 3b and 5b), (iii) by an observed 810 keV γ-ray assigned as cross-over to the 64.6 keV metastable state, and (iv) by the fact that a number of γ-rays (table 3) were seen in common coincidence with the γ-rays at 410, 673 and 810 keV.

The 818 keV γ-ray is in strong coincidence with the 136 keV γ-ray, but not with the 264, 387 or 673 keV γ-rays (figs. 3a,b; 4b and 8a) suggesting a level at 1018.3 keV,

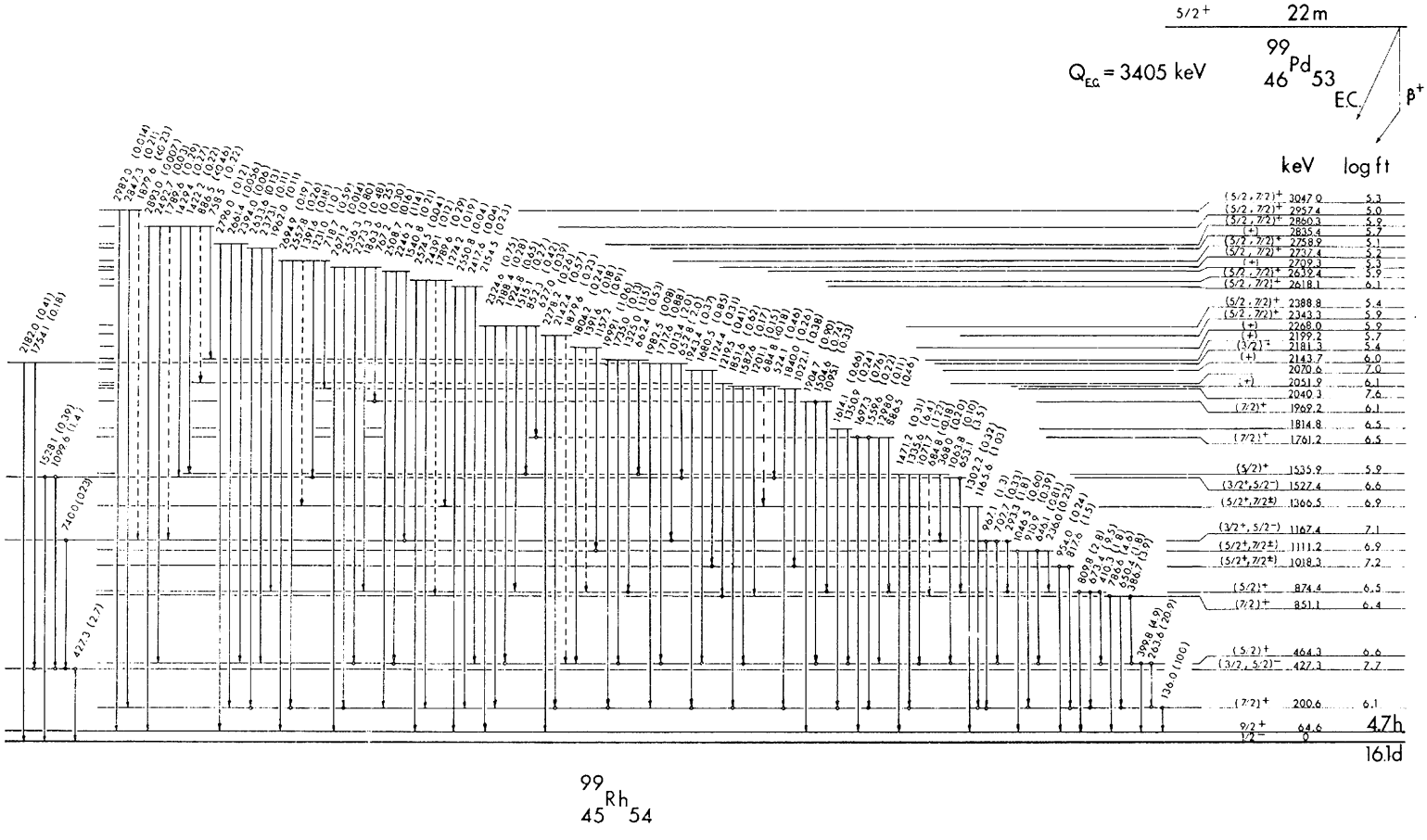

Fig. 10. Proposed decay scheme for 21 min ^{99}Pd. The energies of the γ-rays are given in keV and the intensities in parentheses are relative to the 136 keV γ-ray taken as 100.

which is also supported by a 954 keV γ-ray assigned to populate the 64.6 keV metastable state as it was not seen in coincidence with γ-rays originating from established levels below 1018 keV. The level at 1018.3 keV is further supported by an 818 keV γ-peak observed in coincidence with the energy region 1010-1130 keV in the NaI(Tl) detector (see table 3) probably due to population of this level by the 1022 and 1124 keV γ-rays originating from established levels at higher energy.

The following pairs of γ-rays with an energy difference of 264 keV were seen in coincidence with the 136 and 264 keV γ-rays: 911, 646; 967, 703; 1336, 1072; 1614, 1351; 1852, 1588; 1943, 1681; 1999, 1735 and 2536, 2273 keV (figs. 3a and b). This information strongly supports the assignment of levels at 1111.2, 1167.4, 1535.9, 1814.8, 2051.9, 2143.7, 2199.2 and 2737.4 keV. Additional γ-rays were assigned to depopulate most of these levels either on the basis of observed coincidences or on the basis of energy sums (see fig. 10).

The following pairs of γ-rays with an energy difference of 264 keV were seen in coincidence with the 136 or the 264 keV γ-rays: 1560, 1298; 1983, 1718; 2142, 1880; 2188, 1925; 2509, 2246 and 2634, 2373 keV (figs. 3a and b). This information suggests levels at 1761.2, 2181.3, 2343.3, 2388.8, 2709.3 and 2835.4 keV. Again, additional γ-rays were assigned to depopulate each of these levels on the basis of observed coincidences or energy sums (see fig. 10).

The 653 and 1064 keV γ-rays are in strong coincidence with the 673 and 264 keV γ-rays, respectively (figs. 7c, 8a and 3b). This information establishes a level at 1527.4 keV. Furthermore, the 653 keV γ-ray was observed in strong coincidence with a γ-ray, the energy of which was determined from the coincidence spectra from two experiments to be 652.8 ± 0.5 keV (see fig. 7c). The energy difference between the already established levels at 2181.3 and 1527.4 keV is 652.9 ± 0.6 keV in good agreement with the above value. On this basis, the 652.8 keV γ-ray was assigned to populate the 1527.4 keV level. Interestingly, the 740 and 1100 keV γ-rays are in strong coincidence with the 427 keV γ-ray, while the 653 and 1013 keV γ-rays are in weak coincidence with the 427 keV γ-ray (figs. 5c and 7c). All these observations can be explained by assigning the 427 keV γ-ray to populate the ground state with the 740 and 1100 keV γ-rays populating the 427 keV level directly. These assignments are further strengthened by the 427 and 653 keV γ-ray peaks observed in coincidence with the energy regions 1710-1810 and 1500-1570 keV regions in the NaI detector (containing the 1754 and 1528 keV γ-rays), respectively.

The γ-ray at 1166 keV was seen in coincidence with the 136 keV but not the 264 keV γ-ray. The 1302 keV γ-ray was not seen in any of the coincidence spectra. This information supports a level at 1366.5 keV. This level is further supported by its possible population by γ-rays at 685, 1274 and 1392 keV (see fig. 10).

A level at 1969.2 keV is firmly established by the observed coincidences of the 1095 and 1505 keV γ-rays with the 673 and 136, 264, 400 keV γ-rays, respectively (figs. 8a, 3a and b). The presence of this level also accommodates the 1905 keV γ-ray populating the 64.6 keV isomeric state.

A level at 2040.3 keV is assigned on the basis of the observed coincidence of the 1840 keV γ-ray with 136 keV but not the 264 keV γ-ray (figs. 3a and b) and the possible coincidence of the 1022 keV γ-ray with the 818 keV γ-ray observed in coincidence with the energy region 770-890 keV in the NaI detector.

A possible level at 2070.6 keV is suggested on the basis of the observed coincidence of the 1220 keV γ-ray with the 136, 264, 387 and 400 keV γ-rays (figs. 3a,b, 4b and 5a). No other γ-ray, however, was observed to de-excite this level.

The 1157 keV γ-ray was observed in strong coincidence with the 136, 264 and 400 keV γ-rays (figs. 3a,b and 5a); it was also seen in coincidence with the 630-700 and 1000-1150 keV regions in the NaI detector. This information is consistent with the 1157 keV γ-ray populating the 1111.2 keV level, thus suggesting a level at 2268.0 keV. This is further supported by the 1804 and possibly the 1392 keV γ-rays assigned by energy difference to de-excite this level.

The 2558 keV γ-ray was seen in coincidence with only the 136 keV γ-ray, thus suggesting a level at 2758.9 keV. This level is further supported by the 719, 1231, 2695 and possibly the 1392 keV γ-rays assigned to de-excite this level. The 1231 keV γ-ray was observed in coincidence with the 136 keV γ-ray, and this is consistent with the above assignment.

Finally, levels at 2618.1, 2639.4, 2860.3, 2957.4 and 3047.0 keV are proposed on the basis of at least two energy sums as shown in fig. 10.

The level scheme proposed in fig. 10 accommodates 97.7 % of the total γ-ray intensity and 110 of the 127 γ-rays that were assigned to ^{99}Pd decay.

5. Assignment of J^π values in ^{99}Rh

The Q_{EC} for the decay of ^{99}Pd measured in this work was 3405 ± 20 keV. This value was used in the calculation of the log ft values given in table 4 and is different from the value of 3.82 MeV deduced in ref. [3]) from the value of 2.0 ± 0.1 MeV for the maximum positon energy of Katcoff and Abrash [2]). Column 1 of table 4 gives the energy in keV of the levels assigned to ^{99}Rh; column 2 gives the energy in keV available for electron capture to the levels in ^{99}Rh; column 3 gives the percent population of the levels in ^{99}Rh by β^+ decay and electron capture; column 4 gives the percent of electron capture calculated using the β^+/E.C. ratios given on p. 575 of ref. [4]); column 5 gives the log ft values obtained from these data using the nomogram given on p. 573 of ref. [4]); the last column in table 4 gives the limits for J^π values placed on the basis of the log ft values and on the γ-ray information as discussed below.

As was mentioned in sect. 4, the J^π values for the ground and the metastable states are expected to be $\frac{1}{2}^-$ and $\frac{9}{2}^+$, respectively.

Since many of the beta transitions to levels that are strongly populated have log ft values up to 6.6, it is assumed that these transitions are most likely allowed in character. This limits the J^π values for levels with log ft values less than 6.6 to $(\frac{3}{2}, \frac{5}{2}, \frac{7}{2})^+$. The J^π values can be further limited to $(\frac{5}{2}, \frac{7}{2})^+$ for those levels that were observed to

populate significantly the $\frac{9}{2}^+$ state at 64.6 keV, since a $\frac{3}{2}^+$ assignment would require an M3 transition.

The level at 200.6 keV is strongly populated by β-decay and according to the arguments given above its J^π value is limited to $(\frac{5}{2}, \frac{7}{2})^+$. Level systematics in ^{101}Rh and ^{103}Rh indicate that the $\frac{7}{2}^+$ state should lie low in energy. On this basis, the 200.6 keV level is assigned as $\frac{7}{2}^+$, although a $\frac{5}{2}^+$ value cannot be excluded on the basis of the present information.

TABLE 4

Assignment of log ft and J^π values to levels in ^{99}Rh

Level (keV)		Q_{EC} [a]) (keV)	%(β^++EC)		% EC		log ft	J^π
0								$\frac{1}{2}^-$
64.6	2	3340						$\frac{9}{2}^+$
200.6	2	3204	42.6	11	3.84	10	6.1	$(\frac{7}{2})^+$
427.3	1	2978	0.74	21	0.082	23	7.7	$(\frac{3}{2}, \frac{5}{2})^-$
464.3	2	2941	9.38	96	1.19	11	6.6	$(\frac{5}{2})^+$
851.06	9	2554	7.9	4	1.29	7	6.4	$(\frac{7}{2})^+$
874.39	14	2531	5.1	7	0.85	12	6.5	$(\frac{5}{2}^+)$
1018.28	11	2387	0.87	17	0.17	4	7.2	$(\frac{5}{2}^+, \frac{7}{2}^+)$
1111.2	5	2294	1.25	23	0.27	5	6.9	$(\frac{5}{2}^+, \frac{7}{2}^+)$
1167.4	4	2238	0.81	33	0.18	7	7.1	$(\frac{3}{2}^+, \frac{5}{2}^-)$
1366.5	4	2038	0.81	17	0.22	5	6.9	$(\frac{5}{2}^+, \frac{7}{2}^+)$
1527.4	5	1878	1.34	32	0.45	11	6.6	$(\frac{3}{2}^+, \frac{5}{2}^-)$
1535.86	11	1869	5.65	31	1.93	11	5.9	$(\frac{5}{2})^+$
1761.2	2	1644	0.96	14	0.42	6	6.5	$(\frac{7}{2})^+$
1814.83	15	1590	0.74	8	0.34	4	6.5	
1969.2	1	1436	1.38	17	0.74	9	6.1	$(\frac{7}{2}^+)$
2040.3	1	1365	0.04	13	0.02	8	≈7.6	
2051.9	2	1354	1.23	12	0.74	7	6.1	(+)
2070.6	4	1334	0.15	11	0.09	7	≈7.0	
2143.7	4	1261	1.26	16	0.82	10	6.0	(+)
2181.3	3	1224	4.6	3	3.05	17	5.4	$(\frac{3}{2})^+$
2199.2	3	1206	2.02	10	1.37	7	5.7	+
2268.0	5	1137	1.02	16	0.72	11	5.9	+
2343.3	2	1062	0.78	10	0.59	8	5.9	$(\frac{5}{2}, \frac{7}{2})^+$
2388.8	2	1016	2.23	10	1.73	8	5.4	$(\frac{7}{2})^+$
2618.1	3	787	0.26	6	0.23	5	6.1	$(\frac{5}{2}, \frac{7}{2})^+$
2639.4	5	766	0.41	6	0.37	5	5.9	$(\frac{5}{2}, \frac{7}{2})^+$
2709.3	6	696	1.25	12	1.16	11	5.3	(+)
2737.4	5	668	1.52	19	1.43	18	5.2	$(\frac{5}{2}, \frac{7}{2})^+$
2758.9	3	646	1.76	12	1.66	11	5.1	$(\frac{5}{2}, \frac{7}{2})^+$
2835.4	6	570	0.29	5	0.28	5	5.7	(+)
2860.3	8	545	0.20	3	0.19	3	5.9	$(\frac{5}{2}, \frac{7}{2})^+$
2957.4	3	448	0.93	15	0.92	15	5.0	$(\frac{5}{2}, \frac{7}{2})^+$
3047.0	4	358	0.28	7	0.28	7	5.3	$(\frac{5}{2}, \frac{7}{2})^+$

[a]) The uncertainty in energy is 20 keV for all the listed values.

The level at 427.3 keV is very weakly populated by β-decay and a log ft value of 7.7 suggests a first-forbidden transition with a possible assignment $(\frac{3}{2}, \frac{5}{2}, \frac{7}{2})^-$. This level decays exclusively to the $\frac{1}{2}^-$ ground state, and this excludes the $\frac{7}{2}^-$ as a possibility.

A single proton estimate [p. 578 in ref. [4])] of the intensity ratio (M1, 427 → 0)/(E1, 427 → 201) gives 0.058, which corresponds to an expected intensity of 47 for a 277 keV transition to the 200.6 keV level as compared with an upper limit of ≈ 0.1 obtained from fig. 1. However, E1 transitions in this region may be retarded over the single-proton estimates by a factor of 10^2-10^3 more than M1 transitions, and this may account for the factor of 470 obtained from the upper limit set above. These arguments favor a $\frac{3}{2}^-$ assignment rather than $\frac{5}{2}^-$ for the 427.3 keV level, although the latter cannot be excluded on the basis of the present evidence.

The levels at 851.1, 1761.2, 1969.2 and 2388.8 keV populate rather strongly the $\frac{9}{2}^+$ state at 64.6 keV, and this evidence with reasonable enhancements of E2 versus M1 over the single-proton estimate favors a $(\frac{7}{2})^+$ assignment for these levels. The $(\frac{5}{2})^+$ possibility, however, cannot be excluded as large E2 enhancements, and M1 retardations are not very uncommon in this region.

The 464.3 keV level de-excites strongly to the $(\frac{7}{2})^+$ level at 200.6 keV, and this favors a $(\frac{5}{2})^+$ assignment for this level. Furthermore, the levels at 874.4 and 1535.9 keV strongly populate the $(\frac{7}{2})^+$ and $(\frac{5}{2})^+$ levels at 200.6 and 464.3 keV, respectively, and this evidence points toward a $(\frac{5}{2})^+$ assignment for both these levels.

The level at 1167.4 keV is only very weakly populated by β-decay. As this level does not decay to the $\frac{9}{2}^+$ level at 64.6 keV, we may exclude the $\frac{7}{2}^\pm$ or $\frac{5}{2}^+$ as a possibility. The strong feeding to the $\frac{7}{2}^+$ level at 200.6 keV, on the other hand, helps eliminate the value of $\frac{3}{2}^-$. This level was further observed to populate the $(\frac{3}{2}, \frac{5}{2})^-$ level at 427.3 keV. The present evidence thus limits the J^π value to $\frac{3}{2}^+$ or $\frac{5}{2}^-$ for this level. Similar arguments for the 1527.4 keV level limit the J^π value to $\frac{3}{2}^+$ or $\frac{5}{2}^-$ for this level.

The level at 2181.3 keV is expected to have positive parity since it is strongly populated by β-decay ($\log ft = 5.4$). This level was observed to de-excite strongly to the $\frac{1}{2}^-$ ground state and the $(\frac{3}{2}, \frac{5}{2})^-$ 427.3 keV state. Furthermore this level was not observed to populate the $\frac{9}{2}^+$ 64.6 keV state and populates only very weakly the $\frac{7}{2}^+$ state at 200.6 keV. This evidence strongly suggests an assignment of $\frac{3}{2}^+$ for this level.

The levels at 2343.3, 2618.1, 2639.4, 2737.4, 2758.9, 2860.3, 2957.4 and 3047.0 keV are strongly populated by β-decay and were observed to populate the $\frac{9}{2}^+$ state at 200.6 keV. This limits their assignment to $(\frac{5}{2}, \frac{7}{2})^+$.

The levels at 1018.3, 1111.2 and 1366.5 keV are only weakly populated by β-decay. Since these levels have been observed to populate the $\frac{9}{2}^+$ state at 64.6 keV, the J^π values $\frac{3}{2}^\pm$ and $\frac{5}{2}^-$ can be eliminated as a possibility leaving the values $\frac{5}{2}^+$, $\frac{7}{2}^\pm$ as most likely for these levels.

The levels at 2051.9, 2143.7, 2199.2, 2268.0, 2709.3 and 2835.4 keV are rather strongly populated by β-decay ($\log ft < 6.1$), and they can be assigned as having positive parity. On the basis of the present evidence, the J^π value of these levels can be limited only to $(\frac{3}{2}, \frac{5}{2}, \frac{7}{2})^+$.

Finally, for the levels at 1814.8, 2040.3 and 2070.6 keV, which are only very weakly populated by β-decay ($\log ft \geqq 6.5$), the J^π values cannot be limited any further than $(\frac{3}{2}, \frac{5}{2}, \frac{7}{2})^\pm$.

6. Interpretation of levels in ^{99}Rh

In discussing the nature of the states in odd-mass nuclei with Z or N between 40 and 50, one should distinguish the positive- from the negative-parity states. In this major shell, negative-parity states in odd-mass nuclei arise mainly from filling some of the $p_{\frac{1}{2}}$, $f_{\frac{7}{2}}$ and $p_{\frac{3}{2}}$ states. The positive-parity states, however, may arise from a multi-particle configuration $[(g_{\frac{9}{2}})^{3,5,7}]$ or from the subshells of the next major shell (Z, N, 50 to 82).

Of particular interest in ^{99}Rh are the so-called anomalous $\frac{5}{2}^+$ and $\frac{7}{2}^+$ states [11]), which are observed in odd nuclei with N or Z equal to 43, 45 and 47. The characteristic feature of these anomalous states is that they occur very low in excitation energy, and that they cannot simply be explained by the $[(g_{\frac{9}{2}})^{3,5,7}]_{\frac{5}{2},\frac{7}{2}}$ configuration [11,12]). When the pairing-plus-quadrupole model of Kisslinger and Sorensen [13]) is compared with the region of Tc, Rh and Ag isotopes (Z = 43, 45 and 47) or with the region of odd-mass nucleides with N = 43, 45 or 47, the model appears to break down [11,13,14]). Recently, several attempts have been made to improve and extend the pairing-plus-quadrupole model in order to describe this region of nucleides. Thus Sherwood and Goswami [14]) have extended the quasi-particle phonon coupling theory through the inclusion of correlation effects in the core states and have calculated the lower-lying states in Tc, Rh and Ag isotopes. In the case of the ^{101,103,105}Rh isotopes, the trend of the lower $\frac{9}{2}^+$ states is correctly predicted, and when these results are extended to ^{99}Rh, the $\frac{9}{2}^+$ state may even cross the $\frac{7}{2}^+$ state in agreement with experiment.

In fig. 11, we have summarized the present experimental evidence and some of the calculations for the levels in ^{99,101,103}Rh. From the comparison in fig. 11, it is apparent that the Kisslinger-Sorensen model, although it gives the correct trend for a $\frac{9}{2}^+$ state with neutron number, fails to predict the low-lying $\frac{7}{2}^+$ and $\frac{5}{2}^+$ states, which have been observed experimentally. The Sherwood-Goswami results show the correct positions of the $\frac{7}{2}^+$ and $\frac{9}{2}^+$ levels, but their published results are insufficient for a meaningful comparison with experiment [14]).

Recently Ikegami and Sano in a short communication [5]) have presented preliminary results of an expanded quasi-particle-phonon coupling scheme which included admixtures from the next major shell (e.g. $d_{\frac{5}{2}}$, $g_{\frac{7}{2}}$, $s_{\frac{1}{2}}$ and $d_{\frac{3}{2}}$ from the Z, N, 50-82 major shells). These authors claim to have calculated the levels in the Rh isotopes, but they have published results only for the ^{77,79,81}Se isotopes which agree with experiment only qualitatively [11]).

As $^{79}_{34}Se_{45}$ has 45 neutrons, its level structure may have a formal resemblance with the 45 proton Rh isotopes. For this reason, the results of Ikegami and Sano on ^{79}Se have been included in fig. 11 for comparison. It is important to note that their results for ^{79}Se exhibit many of the observed trends. Thus the energy of the anomalous $\frac{5}{2}^+$ and $\frac{7}{2}^+$ states is lowered substantially with the increasing strength of the phonon-quasiparticle interaction [5]). In contrast to the $\frac{9}{2}^+$ states which are mostly single quasi-particle in the $g_{\frac{9}{2}}$ orbit, the $\frac{5}{2}^+$ and $\frac{7}{2}^+$ are heavily phonon mixed [5]). Before the de-

tailed structure of these anomalous states can be fully understood, specific calculations of the type of Sherwood and Goswami [14]) or of Ikegami and Sano [5]) should be carried out specifically for these Rh isotopes, then more meaningful comparisons with the experimental levels would be possible.

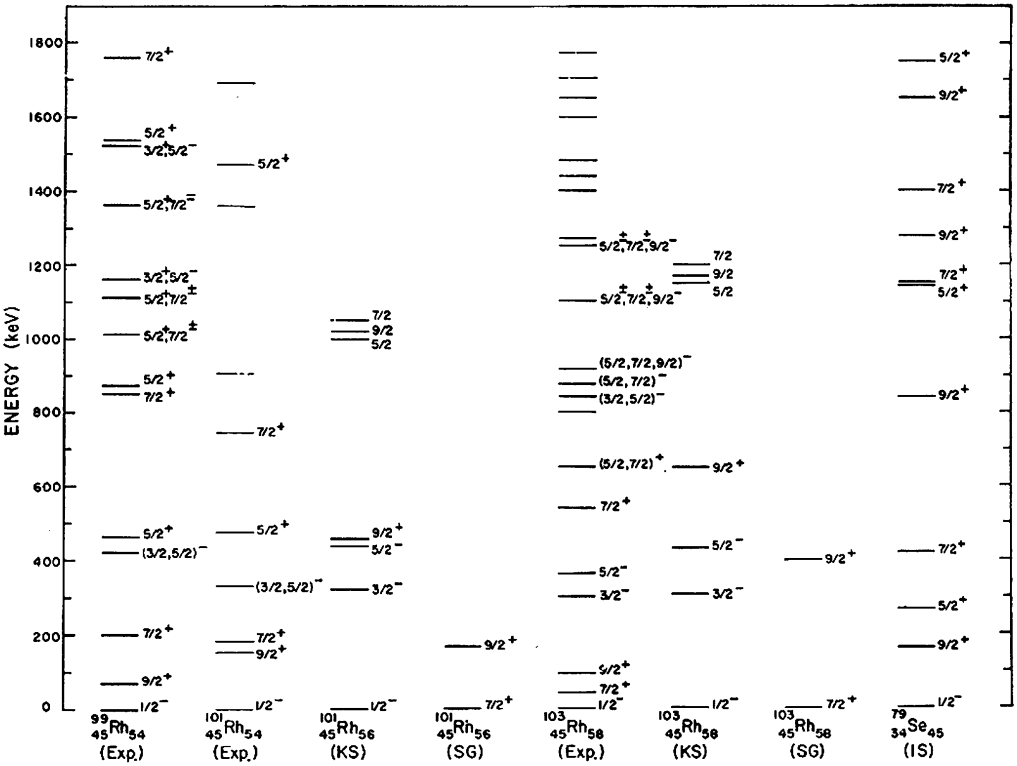

Fig. 11. Comparison of experimental energy levels of the odd-mass Rh isotopes with various theoretical predictions. The levels labeled KS are from ref. [13]), levels SG from ref. [14]) and levels IS from ref. [5]).

Finally, we mention that the low-lying negative-parity states in ^{103}Rh are moderately well predicted by the Kisslinger-Sorensen model [13]), see fig. 11. The low-lying states in ^{103}Rh have been recently investigated by Black, Caelli and Watson [15]) by means of the ^{103}Rh(p, p′) reaction and Coulomb excitation ^{103}Rh(^{16}O, ^{16}O′γ). The J^π assignments from this work are given in fig. 11. Black and coworkers [15]) have interpreted the negative-parity states in ^{103}Rh as originating from the weak coupling of the $\frac{1}{2}^-$ ground state with the one-phonon 2^+ and two-phonon 2^+, 4^+ states of the core. It is, however, apparent that, although these states have substantial collective character, a more realistic description in terms of the pairing-plus-quadrupole model should be applicable here. The quasi-particle-phonon coupling scheme, for example, is more appropriate for the description of these nuclei as it allows for single-quasi-

particle and quasiparticle-phonon coupled amplitudes in the wave function and can naturally account for the observed [15]) M1 decay from the one- or two-phonon coupled states to the ground state. It is further very interesting to contrast the interpretation of Black and coworkers [15]) for ^{103}Rh to that of Engels [6]) for a similar nucleus $^{77}_{34}Se_{45}$. Thus, Engels [6]) has attempted to describe the negative-parity states in ^{77}Se as members of rotational bands following the description of permanently deformed odd-mass nuclei according to the Nilsson model [7]).

In the case of ^{99}Rh, the negative-parity states are not well characterized from the decay of ^{99}Pd as they are not strongly populated by β-decay. Here, in addition to the $\frac{1}{2}^-$ ground state, candidates for the negative-parity states similar to those in ^{103}Rh are the $(\frac{5}{2}, \frac{3}{2})^-$ state at 427.3 keV and conceivably one of the 1018.3, 1111.2, 1167.4, 1366.5 or 1527.4 keV states. From the present information, however, definite conclusions about these states cannot be drawn.

We wish to thank Mr. John Hood and the personnel of the Washington University cyclotron for performing the bombardments. The cooperation of Dr. T. Gallagher and the staff of the Washington University computing facilities is gratefully acknowledged. Finally, we thank Jeanne Teague for typing the manuscript.

References

1) A. H. W. Aten, Jr. and T. DeVries-Hamerling, Physica **19** (1953) 1200
2) S. Katcoff and H. Abrash, Phys. Rev. **130** (1965) 966
3) Nuclear Data Sheets, ed. by K. Way (Academic Press, New York, 1965) p. 729
4) C. M. Lederer, J. M. Hollander and I. Perlman, Table of isotopes sixth ed. (John Wiley and Sons New York, 1967)
5) H. Ikegami and M. Sano, Phys. Rev. Lett. **21** (1966) 323
6) W. Engels, Z. Naturf. **22a** (1967) 2004
7) O. Nathan and S. G. Nilsson, in Alpha-, beta- and gamma-ray spectroscopy, ed. by K. Siegbahn, (North-Holland Publ. Co., Amsterdam, 1965) Chapt. X
8) W. G. Winn and D. G. Sarantites, Nucl. Instr. **66** (1968) 61
9) W. G. Winn and D. G. Sarantites, Phys. Rev., to be published
10) C. W. Townley, J. D. Kurbatov and M. H. Kurbatov, Bull. Am. Phys. Soc. **4** (1959) 366
11) D. G. Sarantites and B. R. Erdal, Phys. Rev. **177** (1969) 1631
12) B. H. Flowers, Proc. Roy. Soc. **215** (1952) 398
13) L. S. Kisslinger and R. A. Sorensen, Revs. Mod. Phys. **35** (1963) 853
14) A. I. Sherwood and A. Goswami, Nucl. Phys. **89** (1966) 465
15) J. L. Black, W. J. Caelli and R. B. Watson, Nucl. Phys. **A125** (1969) 545